Quercetin ameliorates senescence and promotes osteogenesis of BMSCs by suppressing the repetitive element-triggered RNA sensing pathway

YUTONG SUN[1-3*], CHUNYANG WANG[1-3*], LILING WEN[1-3], ZIHANG LING[1-3], JUAN XIA[1-3], BIN CHENG[1-3] and JIANMIN PENG[1-3]

[1]Hospital of Stomatology, Sun Yat-sen University, Guangzhou, Guangdong 510060, P.R. China;
[2]Guangdong Provincial Key Laboratory of Stomatology, Guangzhou, Guangdong 510060, P.R. China;
[3]Guanghua School of Stomatology, Sun Yat-sen University, Guangzhou, Guangdong 510060, P.R. China

Received July 9, 2024; Accepted October 8, 2024

DOI: 10.3892/ijmm.2024.5445

Abstract. Cell senescence impedes the self-renewal and osteogenic capacity of bone marrow mesenchymal stem cells (BMSCs), thus limiting their application in tissue regeneration. The present study aimed to elucidate the role and mechanism of repetitive element (RE) activation in BMSC senescence and osteogenesis, as well as the intervention effect of quercetin. In an H_2O_2-induced BMSC senescence model, quercetin treatment alleviated senescence as shown by a decrease in senescence-associated β-galactosidase (SA-β-gal)-positive cell ratio, increased colony formation ability and decreased mRNA expression of p21 and senescence-associated secretory phenotype genes. DNA damage response marker γ-H2AX increased in senescent BMSCs, while expression of epigenetic markers methylation histone H3 Lys9, heterochromatin protein 1α and heterochromatin-related nuclear membrane protein lamina-associated polypeptide 2 decreased. Quercetin rescued these alterations, indicating its ability to ameliorate senescence by stabilizing heterochromatin structure where REs are primarily suppressed. Transcriptional activation of REs accompanied by accumulation of cytoplasmic double-stranded (ds)RNA, as well as triggering of the RNA sensor retinoic acid-inducible gene I (RIG-I) receptor pathway in H_2O_2-induced senescent BMSCs were shown. Similarly, quercetin treatment inhibited these responses. Additionally, RIG-I knockdown led to a decreased number of SA-β-gal-positive cells, confirming its functional impact on senescence. Induction of senescence or administration of dsRNA analogue significantly hindered the osteogenic capacity of BMSCs, while quercetin treatment or RIG-I knockdown reversed the decline in osteogenic function. The findings of the current study demonstrated that quercetin inhibited the activation of REs and the RIG-I RNA sensing pathway via epigenetic regulation, thereby alleviating the senescence of BMSCs and promoting osteogenesis.

Correspondence to: Professor Bin Cheng or Dr Jianmin Peng, Hospital of Stomatology, Sun Yat-sen University, 56 Lingyuan Road West, Guangzhou, Guangdong 510060, P.R. China
E-mail: chengbin@mail.sysu.edu.cn
E-mail: pengjm9@mail.sysu.edu.cn

*Contributed equally

Key words: bone marrow mesenchymal stem cell, quercetin, cellular senescence, osteogenesis, repetitive element, RIG-I-like receptor pathway

Introduction

Bone marrow mesenchymal stem cells (BMSCs) possess robust self-renewal and multi-lineage differentiation potential, rendering them key cellular resources in bone tissue regeneration engineering (1). However, stress-induced senescence leads to SC exhaustion and a marked decline in osteogenic differentiation, thereby constraining the application of BMSCs (2,3). Therefore, elucidating the specific mechanism underlying BMSC senescence and its impact on SC function, as well as exploring potential intervention strategies, is key.

Cell senescence is a state of cell cycle arrest caused by endogenous and exogenous stimuli, accompanied by epigenetic changes (4). The observed alterations include disruption of heterochromatin structure (5), aberrations in DNA methylation and histone modification patterns (6), as well as perturbations in nuclear membrane integrity (7). ~50% of eukaryotic genome sequences are repeats and organized into densely packed and transcriptionally suppressed heterochromatin (8,9). Under certain pathophysiological conditions, such as cancer, placental development and aging, heterochromatin is reorganized by epigenetic modification and accompanied by aberrant transcriptional activation of repetitive elements (REs) (10-12). REs are classified into tandem and interspersed repeats based on structural organization. Tandem repeats consist of satellite and simple repeats, while interspersed REs primarily refer to transposable elements that actively or passively integrate into the genome. Transposable elements are divided into RNA (class I) and DNA transposons (class II elements) according to the transposition mechanisms. DNA

transposons mobilize their DNA sequence through a 'cut and paste' process, wherein transposons are excised from the donor site and inserted into a different genomic location (13). By contrast, retrotransposons mobilize via a 'copy and paste' manner, which involves reverse transcription of an RNA intermediate followed by insertion into a new locus (14). Retrotransposons are categorized into two subtypes: Long terminal repeats (LTRs) and non-LTRs. LTRs are commonly known as endogenous retroviruses (ERVs), whereas non-LTRs include long interspersed nuclear elements (LINEs) and short interspersed nuclear elements (15,16). Due to their presence in the host genome but transcriptional silencing, REs have been regarded as 'junk DNA'. However, advancements in sequencing and computer analysis technologies have led to a re-evaluation of REs, particularly transposable elements, enabling more comprehensive exploration of their biological functions (17). RE transcription leads to accumulation of endogenous cytosolic self-nucleic acids, potentially leading to the activation of intracellular signaling pathways (18-20). Epigenetic resetting and RE activation during aging and senescence have been reported (11), however, the internal mechanisms by which they affect the senescence and function of BMSCs remain poorly understood.

Quercetin, a natural bioactive flavonoid extracted from a wide variety of fruits, vegetables is known for its anti-inflammatory, antioxidant and anti-cancer properties (21,22). Quercetin is a well-established senolytic drug that effectively targets multiple mechanisms to eliminate senescent cells and suppress the senescence-associated secretory phenotype (SASP) (23). The activities of this compound are associated with activation of various pathways, including the PI3K/Akt and AMPK pathways, and sirtuin 1/PINK1/Parkin-mediated mitophagy (21). However, the extent to which quercetin can mitigate or reverse senescence-related decline of BMSC function and its potential role in regulating epigenetic mechanisms and inhibiting activation of REs remain largely unexplored.

The present study investigated the effect of quercetin against oxidative stress-induced senescence of BMSCs and its role in reversing senescence-associated decline in osteogenic capacity. The current study aimed to provide new ideas for the intervention of SC senescence and development of bone tissue regeneration.

Materials and methods

Isolation and culture of BMSCs. Animal experiments were conducted according to the approved guidelines for experimental animal ethics and welfare by the Institutional Animal Care and Use Committee of Sun Yat-Sen University (Guangzhou, China) (approval no. SYSU-IACUC-2024-002262). For BMSC isolation, 10 3-week-old male Sprague-Dawley rats weighing about 50 g were purchased from the Laboratory Animal Center of Sun Yat-Sen University. Rats were sacrificed by cervical dislocation under anesthetization with isoflurane inhalation (induction, 3%; maintenance, 2%). Animal death was confirmed by respiratory arrest, cessation of heartbeat and disappearance of reflexes. Rats were immersed in 75% ethanol at room temperature for 20 min to sterilize. Tibiae and femurs were dislocated and both ends were cut off under aseptic conditions. The bone marrow was flushed out using a syringe, cut into small fragments and subsequently collected by centrifugation (250 x g, 5 min, 4˚C). The fragments were resuspended in DMEM (Gibco; Thermo Fisher Scientific, Inc.) and seeded into a culture flask. Primary BMSCs were cultured in DMEM containing 10% fetal bovine serum (Moregate BioTech) and 100 μg/ml Primocin® (InvivoGen) in a humidified incubator containing 5% CO_2 at 37˚C. The culture medium was changed every 3 days. Passage three BMSCs were used for subsequent experiments.

Chemical compounds. Quercetin was purchased from MedChemExpress and dissolved in DMSO (Sigma-Aldrich; Merck KGaA). Poly(I:C)-LMW/LyoVec™ [Poly(I:C)], was purchased from InvivoGen and dissolved following the manufacturer's instructions. Briefly, to prepare a stock solution (50 μg/ml), 25 μg lyophilized Poly(I:C) was added to 500 μl endotoxin-free water and gently mixed for ≥15 min. The products were aliquoted and stored at -20˚C.

Osteogenic differentiation. For osteogenic induction, BMSCs ($1.5x10^5$ cells/well) were seeded in 12-well plates. After reaching 70-80% confluence, cells were stimulated with 200 μM H_2O_2 for 1 h or treated with 0.1 μg/ml Poly(I:C) for 24 h at 37˚C with 5% CO_2. Cells were washed and cultured with osteogenic induction medium (Cyagen Biosciences Inc.) at 37˚C with 5% CO_2. Quercetin at concentration of 1 μM was added to osteogenic induction medium. The culture medium was refreshed every 3 days. Alkaline phosphatase (ALP) staining was conducted after 7 days using a BCIP/NBT ALP Color Development kit (Beyotime Institute of Biotechnology) according to the manufacturer's instructions. Alizarin red staining was performed 14-21 days post-induction. Briefly, BMSCs were washed with PBS and fixed with 4% paraformaldehyde at room temperature for 30 min. Cells were stained with alizarin red for 10 min at room temperature. After that, the images were captured by an inverted light microscope (Zeiss Axio; magnification, x100). The stained area was calculated by Image J 1.48v software (National Institutes of Health).

Treatment and transfection. To assess the geroprotective effect of quercetin treatment and RIG-I knockdown, $2x10^4$ BMSCs were seeded in 24-well plates and cultured at 37˚C with 5% CO_2 in complete DMEM for 24 h. Next, cells were treated with 200 μM H_2O_2 for 1 h to induce senescence. For quercetin treatment, cells were washed with phosphate-buffered saline (PBS) and cultured with fresh complete DMEM containing quercetin (0.0, 0.1, 1.0, 10.0 and 100.0 μM) at 37˚C with 5% CO_2 for 3 days. For RIG-I knockdown, cells were washed and subjected to short-interfering RNA (siRNA) transfection using Lipofectamine® RNAiMAX Reagent (Invitrogen; Thermo Fisher Scientific, Inc.; cat. no. 13778-150) according to the manufacturer's instructions. Briefly, cells were transfected with 50 nM siRNA at 37˚C with 5% CO_2 for 6 h. The si-RIG-I (5'-CAUUGAAACCAAGAAAUUACC-3') were synthesized by GENEray Biotech (Shanghai) Co., Ltd. The si-negative control (NC, 5'-UUCUCCGAACGUGUCACGUTT-3') was set as the control. To evaluate knockdown efficiency, cells were harvested for qPCR 48-72 h after transfection.

Senescence-associated β-galactosidase (SA-β-gal) staining. Following treatment with quercetin at 37˚C with 5% CO_2 for 3 days, senescent cells were assessed using a SA-β-gal staining kit (Beyotime Institute of Biotechnology) according to manufacturer's instructions. Briefly, cultured cells were fixed at room temperature for 15 min, washed with PBS and incubated with staining solution at 37˚C overnight. Images were captured using an inverted light microscope (Zeiss Axio; magnification, x100) and the ratio of stained cells was quantified using ImageJ 1.48v software (National Institutes of Health).

Cell Counting Kit-8 (CCK-8) assay. The optimal concentration of quercetin was selected by assessing its toxic effect using CCK-8 assay. Briefly, BMSCs ($3x10^3$ cells/well) were seeded in 96-well plates and treated with quercetin (0.0, 0.1, 1.0, 10.0, 100.0 and 1,000.0 μM) at 37˚C with 5% CO_2. After 3 days, cell viability was measured using CCK-8 (Dojindo Laboratories, Inc.) according to the manufacturer's protocol. Briefly, cells were incubated with CCK-8 solution for 2 h at 37˚C. Quercetin concentrations that significantly decreased cell viability compared with the blank control were considered cytotoxic.

Colony formation assay. The colony formation assay was used to evaluate the self-renewal ability of BMSCs. In brief, $5x10^3$ BMSCs were seeded in 12-well plates and stimulated with 200 μM H_2O_2 to induce senescence as aforementioned. Then, BMSCs were cultured in complete DMEM (Gibco; Thermo Fisher Scientific, Inc.) at 37˚C with addition of quercetin (0.0, 0.1, 1.0, 10.0 and 100.0 μM) for 7-10 days. The number of colonies formed was calculated by crystal violet staining (Beijing Solarbio Science & Technology Co., Ltd.). Briefly, cells were fixed with 4% paraformaldehyde for 15 min, then stained with 0.1% crystal violet for 15 min, both at room temperature. The images were captured and the number of colonies (>50 cells) were manually calculated.

Reverse transcription-quantitative PCR (RT-qPCR). After culturing in DMEM or osteogenic induction medium (Cyagen Biosciences Inc.), total RNA was extracted from cells using the RNA-Quick Purification kit (cat. no. RN001; Yishan Biotechnology Co., Ltd.). RNA was reverse-transcribed into cDNA using HiScript II Q RT SuperMix according to the manufacturer's protocol for qPCR (Vazyme Biotech Co., Ltd.). qPCR was performed using Taq Pro Universal SYBR qPCR Master Mix (Vazyme Biotech Co., Ltd.) on a Light Cycler 480 system (Roche Applied Science). The thermocycling conditions were as follows: Initial denaturation at 95˚C for 30 sec, followed by 40 cycles of denaturation at 95˚C for 10 sec, annealing and extension at 60˚C for 30 sec; and a melting curve between 60 and 95˚C. All results were normalized to GAPDH and the quantitative method of relative mRNA expression was used $2^{-\Delta\Delta Cq}$ (24). The senescence marker gene (p21), SASP genes (IL6, TNF-α, IL1α and IL1β), and osteogenic marker genes [osteoprotegerin (OPG), osteocalcin (OCN), osteopontin (OPN) and type I collagen α 1 (COL1A1)] were detected. The PCR primers are listed in Table I.

Cellular immunofluorescence. BMSCs ($2x10^4$ cells/well) were seeded on slides in 24-well plates. Following senescence induction and quercetin treatment, cellular immunofluorescence was used to evaluate expression of γ-H2AX, methylation histone H3 Lys9 (H3K9me3), heterochromatin protein 1α (Hp1α), lamina-associated polypeptide 2 (LAP2), double-stranded (ds)RNA clone rJ2 (rJ2), LINE-1 open reading frame 1 protein (ORF1p) and dsDNA. BMSCs cultured on microscope coverslips at 37˚C for 3 days were fixed with 4% paraformaldehyde for 15 min, permeabilized with 0.4% Triton X-100 in PBS for 30 min and blocked with 10% goat serum (BOSTER Biological Technology Co., Ltd.) for 1 h, all at room temperature. Slides were covered with primary antibodies at 4˚C overnight followed by the Alexa Fluor 488 dye-(1:300; cat. no. EM35141-01; Beijing Emarbio Science & Technology Co., Ltd.) or Alexa Fluor 594 dye-conjugated secondary antibodies (1:300; cat. no. EM35150-01; Beijing Emarbio Science & Technology Co., Ltd.) for 1 h at room temperature in the dark. Nuclei were stained with DAPI for 10 min at room temperature and slides were mounted using anti-fading mounting medium (Vector Laboratories, Inc.; cat. no. H-1000). Images were acquired using a laser scanning confocal microscope (Carl Zeiss AG; magnification, x400). The mean immunofluorescence intensity or proportion of positive cells was quantified using ImageJ 1.48v software.

Table I. Sequences for PCR.

Gene	Sequence, 5'→3'
p21	F-TGTGATATGTACCAGCCACAGG
	R-GCGAAGTCAAAGTTCCACCG
IL6	F-CTGCTCTGGTCTTCTGGAGT
	R-GGTCTTGGTCCTTAGCCACT
TNF-α	F: GGCGTGTTCATCCGTTCTCT
	R: CCCAGAGCCACAATTCCCTT
IL1α	F: AGGGCACAGAGGGAGTCAA
	R: AGAGACAGATGGTCAATGGCA
IL1β	F: GGGATGATGACGACCTGCTA
	R: TGTCGTTGCTTGTCTCTCCT
OPG	F: TGTCCCTTGCCCTGACTACT
	R: GTAGCGCCCTTCCTCACATT
OCN	F: CCGTTTAGGGCATGTGTTGC
	R: CCGTCCATACTTTCGAGGCA
OPN	F: AAGCGTGGAAACACACAGC
	R: CTTTGGAACTCGCCTGACTG
COL1A1	F: GAGACAGGCGAACAAGGTGA
	R: GGGAGACCGTTGAGTCCATC
RIG-I	F: AGCCAATGCGTTCTTACCCA
	R: CATCGCCGAGTGCTAAGAGT
IFN-β	F: AGCACTGGGTGGAATGAGAC
	R: GACCACCATCCAGGCATAGC
GAPDH	F: TATGACTCTACCCACGGCAAG
	R: TACTCAGCACCAGCATCACC

F, forward; R, reverse; OPG, osteoprotegerin; OCN, osteocalcin; OPN, osteopontin; COL1A1, type I collagen α1; RIG-I, retinoic acid-inducible gene I.

The antibodies used for immunofluorescence staining were as follows: γ-H2AX (1:400; cat. no. 9718; Cell Signaling Technology, Inc.), H3K9me3 (1:400; cat. no. ab8898; Abcam), Hp1α (1:200; cat. no. 2616; Cell Signaling Technology, Inc.), LAP2 (1:100; cat. no. 611000; BD Biosciences), rJ2 (1:100; cat. no. MABE1134; MilliporeSigma), ORF1p (1:200; cat. no. MABC1152; MilliporeSigma) and dsDNA (1:400; cat. no. sc-58749; Santa Cruz Biotechnology, Inc.).

Western blotting. BMSCs ($3x10^5$ cells seeded in 6-well plates) were lysed in RIPA buffer (Beyotime Institute of Biotechnology) supplemented with protease and phosphatase inhibitors. Total protein was quantified using BCA Protein Assay kit (Bio-Rad Laboratories, Inc.). Then, 30 μg/lane protein were loaded onto SDS-PAGE in 5-15% Bis-Tris precast gel to separate the different proteins. Subsequently, samples were transferred to a PVDF membrane (MilliporeSigma) and blocked with 5% non-fat milk for 1 h at room temperature. Then, PVDF membranes were incubated with primary antibodies [H3K9me3, Hp1α, LAP2, RIG-I, phosphorylated TANK-binding kinase 1 (p-TBK1), TBK1 or GAPDH] at 4˚C overnight followed by secondary antibodies (1:10,000; HRP AffiniPure Goat Anti-Rabbit, cat. no. EM35111-01 or HRP AffiniPure Goat Anti-Mouse, cat. No. EM35110-01; Beijing Emarbio Science & Technology Co., LTD.) for 1 h at room temperature. The signals were detected using the ECL Immobilon Western Chemilum HRP Substrate (cat. no. WBKLS0500; Merck Millipore) and an ultra-high sensitivity chemiluminescence imaging system (Bio-Rad Laboratories, Inc.) and then quantified using ImageJ 1.48v software (National Institutes of Health).

The antibodies were as follows: H3K9me3 (1:1,000; cat. no ab8898; Abcam), Hp1α (1:1,000; cat. no. 2616; Cell Signaling Technology, Inc.), LAP2 (1:500; cat. no. 611000; BD Biosciences), RIG-I (1:1,000; cat. no. A13407; ABclonal Biotech Co., Ltd.), p-TBK1 (1:250; cat. no. AP1418; ABclonal Biotech Co., Ltd.), TBK1 (1:1,000; cat. no. A3458; ABclonal Biotech Co., Ltd.) and GAPDH (1:3,000; cat. no. 60004-1-Ig; Proteintech Group, Inc.).

RNA sequencing (RNA-seq) and data processing. Following H_2O_2 stimulation and quercetin treatment, RNA-seq analysis of BMSCs was conducted by Shanghai Majorbio Bio-pharm Technology Co., Ltd. Total RNA was obtained using MJZol total RNA extraction kit (cat. no. T01-500; Majorbio). RNA quality was determined by 5300 Bioanalyzer (Agilent) and quantified using ND-2000 (NanoDrop Technologies). The loading concentration of the final library was 10 pM. Agarose gel (Biowest Agarose; Biowest) electrophoresis was used to detect the RNA integrity. mRNA was enriched with Oligo (dT) beads, fragmented into short fragments (300 bp), and reverse-transcribed into cDNA. After being linked to adaptor and purified, cDNA fragments were sequenced on an Illumina NovaSeq Xplus platform (Illumina, Inc.). cDNA library was prepared following Illumina® Stranded mRNA Prep, Ligation (cat. no. 20040534; Illumina, Inc.). The sequencing library was performed on NovaSeq X plus platform (PE150) using NovaSeq X Series 10B Reagent Kit (300cycles; cat. no. 20085594; Illumina Inc.) and 300 bp paired-end reads were generated. The cleaned reads were mapped to *Rattus norvegicus* genome (mRatBN7.2; ncbi.nlm.nih.gov/datasets/genome/GCF_015227675.2) using hisat2 (version 2.1.0). For RE analysis, transposable elements were quantified and analyzed using TE transcripts (version 2.2.3). Differentially expressed REs were counted using R package DESeq2 (version 1.38.2) with a cut-off of $|\log_2(\text{fold change})| > 0.3$ and $P<0.05$. The genes significantly affected by H_2O_2 stimulation or quercetin were determined by setting a fold change of ≥1.5 and $P<0.05$. Venn diagram analysis of differentially expressed genes, Kyoto Encyclopedia of Genes and Genomes (KEGG) pathway and Gene Set Enrichment Analysis (GSEA) were performed on Majorbio Cloud (majorbio.com).

Statistical analysis. The data are presented as the mean ± standard deviation of three independent experimental repeats. Results were statistically analyzed using GraphPad Prism (version 5.0; Dotmatics). Comparisons were conducted with unpaired Student's t-test or one-way ANOVA followed by Dunnett's post hoc test. $P<0.05$ was considered to indicate a statistically significant difference.

Results

Quercetin alleviates oxidative stress-induced senescence in BMSCs. The accumulation of reactive oxygen species in BMSCs causes oxidative stress-induced senescence and impairs SC properties (25). To induce cellular senescence in the present study, exogenous H_2O_2 was used to stimulate BMSCs. Following treatment with 200 μM H_2O_2, the proportion of SA-β-gal-positive cells significantly increased (Fig. 1A and B), indicating cellular senescence was successfully induced under this condition. To investigate the effect of quercetin on senescent BMSCs, quercetin (0, 0.1, 1, 10 and 100 μM) were used to treat H_2O_2-induced BMSCs for 72 h. The ratio of SA-β-gal-positive cells was reduced with an increase in quercetin concentration, especially when the concentration >1 μM (Fig. 1A and B). Additionally, uninduced BMSCs were treated with quercetin to assess cytotoxicity. Quercetin had no significant effect on cell viability at concentrations of 0.0, 0.1, 1.0 and 10.0 μM. However, it exerted toxic effects on BMSCs when the concentration reached 100 and 1,000 μM (Fig. 1C). To identify the optimal concentration, the restorative effect of quercetin on proliferation of senescent BMSCs was further investigated. The colony formation assay demonstrated the impaired proliferative ability of senescent BMSCs was rescued by quercetin at 1 μM (Fig. 1D and E). Consequently, subsequent experiments were conducted using this concentration. H_2O_2 resulted in upregulation of p21 mRNA expression, which was decreased upon treatment with quercetin (Fig. 1F). Senescent cells do not divide but retain the ability to secrete bioactive molecules known as SASP, which alters the microenvironment for both senescent and surrounding cells (26). SASP-associated IL6, TNF-α, IL1α and IL1β showed increased mRNA expression following H_2O_2 treatment; however, expression decreased following quercetin treatment (Fig. 1G). These data aligned with the SA-β-gal staining and colony formation results showing that quercetin alleviated cellular senescence phenotype induced by H_2O_2.

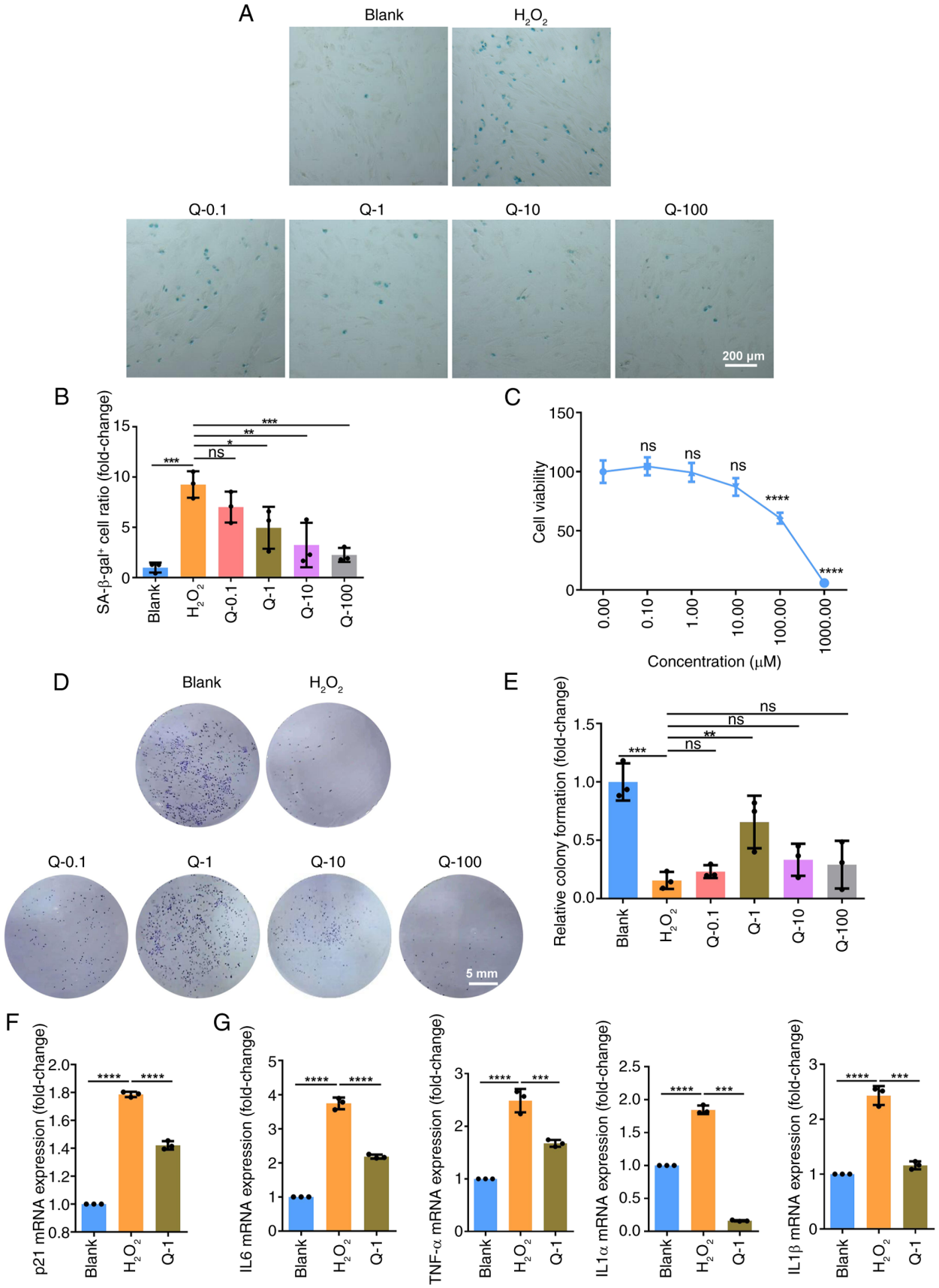

Figure 1. Optimal concentration of Q for alleviating senescence in BMSCs. (A) BMSCs were exposed to 200 μM H_2O_2 for 1 h to induce senescence, followed by treatment with Q for 3 days. Subsequently, SA-β-gal staining was performed. (B) Ratio of senescent cells was quantitatively analyzed. (C) Cell Counting Kit-8 assay was conducted to evaluate the cytotoxic effects of Q on BMSCs. (D) Colony formation assay and (E) quantitative analysis were used to investigate the effect of Q on proliferation of senescent BMSCs. (F) Reverse transcription-quantitative PCR was used to detect mRNA expression levels of the senescence marker p21 as well as those of the senescence-associated secretory phenotype-associated (G) IL6, TNF-α, IL1α and IL1β. Data were quantified as fold-change. *P<0.05, **P<0.01, ***P<0.001, ****P<0.0001 vs. H_2O_2. ns, non-significant; BMSC, bone marrow mesenchymal stem cell; SA-β-gal, senescence-associated β-galactosidase; Q, quercetin.

Quercetin restores genomic and epigenomic instability in senescent BMSCs. The instability of the genome caused by persistent DNA damage and accumulating mutations, along with epigenomic instability characterized by loss of heterochromatin structure and RE suppression are mechanisms underlying senescent phenotypes (27). The dsDNA break marker γ-H2AX is a notable molecular indicator for DNA damage and serves as a hallmark of genomic instability (28). Immunofluorescence revealed a significant increase in nuclear γ-H2AX signal in H_2O_2-induced senescent BMSCs. Quercetin resulted in a reduced expression of γ-H2AX, demonstrating that quercetin stabilized the genome of BMSCs (Fig. 2A). In eukaryotic cells, most of the genome is packaged into condensed and transcriptionally suppressed heterochromatin. H3K9me2 and 3 are epigenetic markers of heterochromatin found on transposable elements to ensure their transcriptional suppression (29). There was a noticeable decrease in expression of H3K9me3 in H_2O_2-induced senescent BMSCs; however, this decrease was rescued by quercetin (Fig. 2B). Consistently, western blotting demonstrated a decrease in expression of H3K9me3 in H_2O_2-induced senescent BMSCs, which was rescued by quercetin (Fig. 2E). The HP1 family binds to H3K9me2 and 3 and interacts with other proteins to maintain chromatin condensation (30). Both immunofluorescence staining and western blotting revealed that Hp1α expression decreased in the H_2O_2 group but recovered in the quercetin group (Fig. 2C and E). Additionally, LAP2, involved in the compaction of heterochromatin by anchoring it on the inner nuclear membrane (30), exhibited similar expression patterns as H3K9me3 and Hp1α and was downregulated in the H_2O_2 but rescued in the quercetin group (Fig. 2D and E). These data demonstrated a decrease in the structural integrity of heterochromatin during senescence, with quercetin serving a key role in safeguarding genomic and epigenomic stability, thereby mitigating senescence.

Quercetin ameliorates senescence by inhibiting the activation of REs and accumulation of cytoplasmic dsRNA in BMSCs. Loss of suppressive epigenetic regulation and heterochromatin structure during cell senescence process may elicit transcriptional activation of REs (9). To elucidate the mechanism by which quercetin alleviates senescence of BMSCs, bulk mRNA sequencing was employed to assess the transcriptional levels of REs. A total of 176 REs was differentially expressed after H_2O_2 treatment. All differentially expressed REs were transcribed at elevated levels in H_2O_2-induced senescent BMSCs. Quercetin resulted in differential expression of 15 repeated sequences in senescent BMSCs, among which 86.67% (13/15) were downregulated (Fig. 3A). To identify REs upregulated by H_2O_2 and rescued by quercetin, Venn diagram analysis was used. The rescued REs primarily included the LINE-1 and ERV families (Fig. 3B). The heatmap revealed augmented expression of these REs in the H_2O_2 group, whereas downregulation was observed in the quercetin group, suggesting the involvement of LINE-1 and ERVs in quercetin-mediated alleviation of cell senescence (Fig. 3C). Activation of RE transcription results in translocation of endogenous RNA to the cytoplasm and generation of DNA through reverse transcriptase activity (31). Immunofluorescence using rJ2 antibody confirmed the accumulation of cytosolic dsRNA in senescent BMSCs. Quercetin decreased the proportion of cytoplasmic rJ2-positive BMSCs (Fig. 3D and E). In accordance with endogenous expression of dsRNA, there was elevated cytoplasmic protein expression of LINE-1 ORF1p in H_2O_2-induced senescent BMSCs, which was be reversed by administration of quercetin (Fig. 3F and G). RNA derived from retroelements can also be converted to dsDNA in cytoplasm through endogenous reverse transcriptase activity; however, no cytoplasmic dsDNA was detected in any group, indicating that dsDNA was not involved in the mechanism underlying H_2O_2-induced BMSC senescence (Fig. 3H).

Induction of dsRNA triggers RIG-I receptor signaling and innate immune response activation, whereas quercetin inhibits this process. Endogenous cytosolic self-nucleic acids can directly trigger innate immune receptor signaling and induce inflammatory responses via recognition of RNA or DNA (15,20). To identify the downstream effect of dsRNA, Venn diagram analysis was employed to identify quercetin-rescued genes that exhibited differential expression in response to H_2O_2 and displayed similar expression patterns as dsRNA transcripts. A total of 20 genes were upregulated by H_2O_2 and differential expression was reversed by quercetin (Fig. 4A). KEGG analysis revealed that these genes were significantly enriched in pathways including 'viral protein interaction with cytokine and cytokine receptor', 'cytosolic DNA-sensing pathway', 'RIG-I-like receptor signaling pathway' and 'toll-like receptor signaling pathway' (Fig. 4B), which are associated with innate immune response. Moreover, GSEA demonstrated activation of innate immune response in H_2O_2-induced senescence of BMSCs (Fig. 4C). RIG-I-like receptor signaling pathway serves a key role in recognizing cytoplasmic dsRNA and initiating an IFN response. To validate the activation of this pathway, western blotting was performed, revealing H_2O_2 treatment upregulated expression of RIG-I and innate immunity-related protein p-TBK1. Conversely, quercetin downregulated these proteins (Fig. 4D and E). To investigate the role of RIG-I-like receptor signaling pathway in senescence induction, siRNA was used to knock down RIG-I expression in rat-derived BMSCs. The effectiveness of knockdown was confirmed by RT-qPCR and western blotting (Fig. 4F). RIG-I knockdown resulted decreased expression of downstream innate immune effector IFN-β which was upregulated in H_2O_2-induced senescence (Fig. 4G). SA-β-gal staining was used to assess cell senescence. Notably, RIG-I knockdown led to a decrease in the proportion of SA-β-gal-positive cells following H_2O_2 treatment, thereby confirming the functional impact of RIG-I on cell senescence (Fig. 4H and I). Overall, the present findings suggested that cytoplasmic dsRNAs induced by REs contributed to activation of RIG-I receptor signaling and subsequent innate immune response. This activation lead to type I IFN response and proinflammatory cytokine production, ultimately promoting senescence.

Quercetin promotes osteogenesis in senescent BMSCs by inhibiting the dsRNA-induced RIG-I receptor signaling pathway. To evaluate the effect of quercetin on osteogenic differentiation potential of senescent BMSCs, BMSCs were cultured in an osteoblast differentiation medium for 7-21 days. Oxidative stress-induced senescence impaired osteogenic potential of

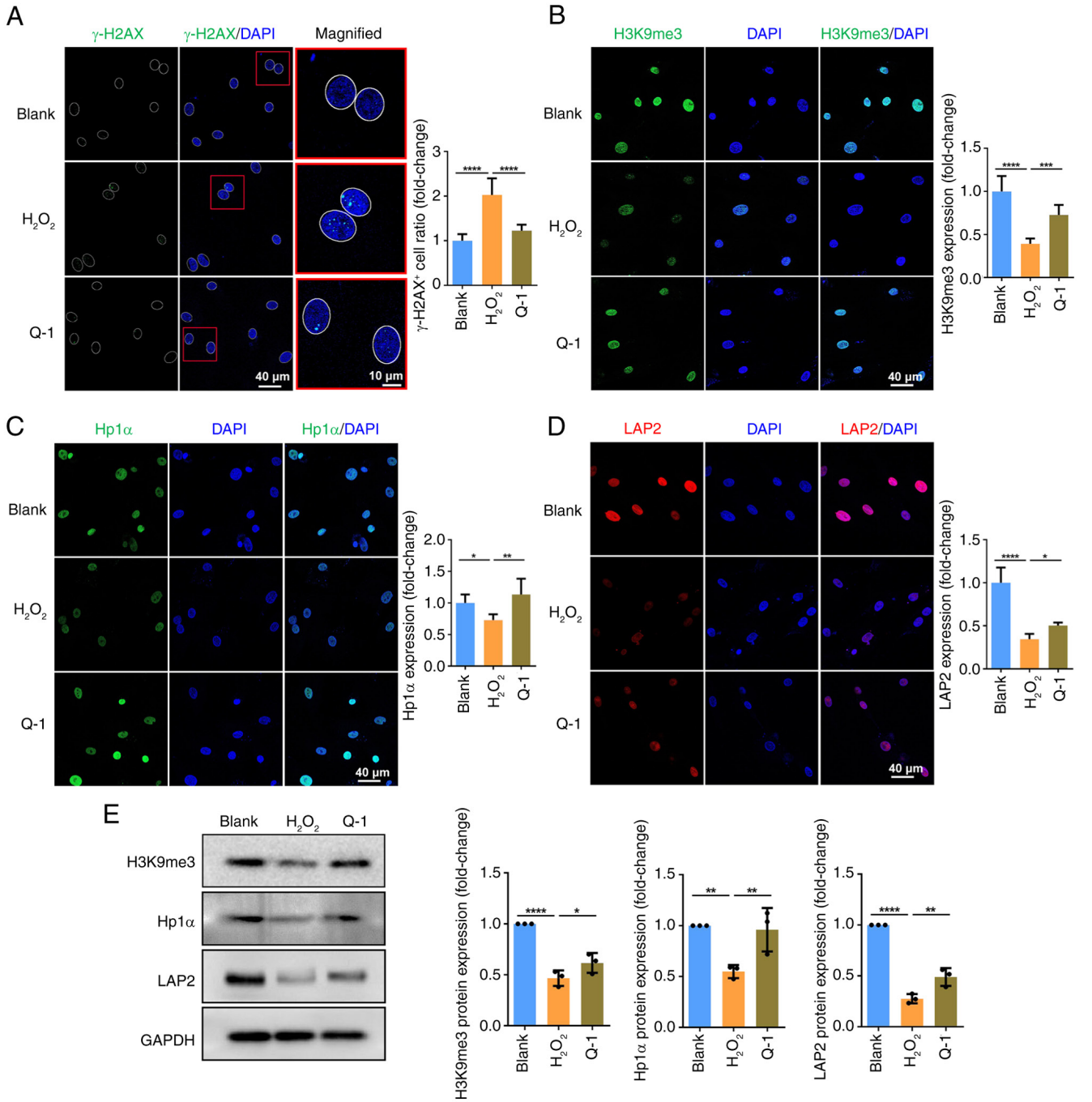

Figure 2. Q decreases DNA damage response and restores epigenetic characteristics of senescent BMSCs. Immunofluorescence staining of (A) γ-H2AX, (B) H3K9me3, (C) Hp1α and (D) LAP2 was performed in BMSCs. (E) Western blotting of H3K9me3, Hp1α and LAP2 protein expression in BMSCs. Data were quantified as fold-change. *P<0.05, **P<0.01, ***P<0.001, ****P<0.0001. BMSC, bone marrow mesenchymal stem cell; H3K9me3, methylation histone H3 Lys9; LAP2, lamina-associated polypeptide 2; Hp1α, heterochromatin protein 1α; Q, quercetin.

BMSCs, as indicated by a decrease in ALP and alizarin red staining. However, quercetin restored the osteogenic differentiation ability of senescent BMSCs (Fig. 5A and B). The results were further supported by RT-qPCR of osteogenic marker genes, including OPG, OCN, OPN and COL1A1. mRNA levels of osteogenic marker genes (OPG, OCN, OPN, COL1A1) were decreased in senescent BMSCs, whereas they increased after quercetin administration (Fig. 5C). The aforementioned results demonstrated that dsRNA contributes to the mechanism by which quercetin ameliorates BMSC senescence. Furthermore, the role of dsRNA and downstream RIG-I receptor signaling pathway was investigated by adding synthetic dsRNA analogue Poly(I:C), which activates the RIG-I signaling pathway, to the osteoblast differentiation medium. Poly(I:C) resulted in a concentration-dependent decrease in alizarin red staining (Fig. 6A), confirming that dsRNA decreased osteoblast differentiation potential of BMSCs. Moreover, the positive area of alizarin red staining improved with si-RIG-I compared with the si-NC control (Fig. 6B), indicating knockdown of RIG-I partially rescued the impaired osteoblast differentiation ability of BMSCs caused by dsRNA. Similarly, knockdown of RIG-I improved osteogenic differentiation ability of BMSCs impaired

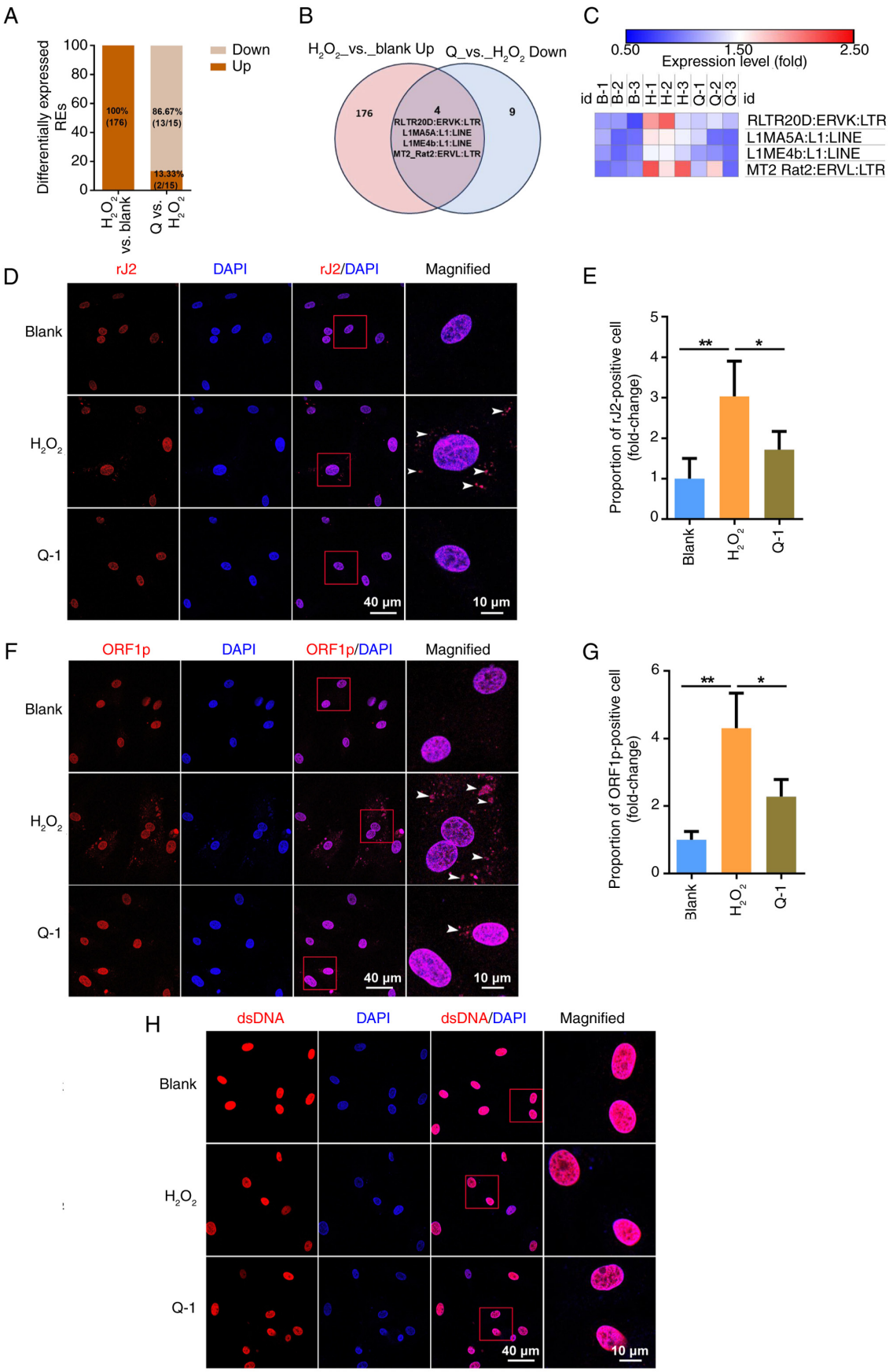

Figure 3. Q inhibits activation of REs and accumulation of cytoplasmic dsRNA in senescent BMSCs. (A) Transcription levels of REs were analyzed by RNA-seq. (B) Venn diagram was used to identify the overlapping REs that were upregulated by H_2O_2 induction and reversed by Q. (C) Expression heatmap depicting the overlapping REs. (D) Immunofluorescence staining of rJ2 was performed in BMSCs. (E) Cytoplasmic rJ2-positive cells was quantified. (F) Immunofluorescence staining of ORF1p was performed in BMSCs. (G) Proportion of cytoplasmic ORF1p-positive cells was quantified. (H) Immunofluorescence staining of dsDNA was performed in BMSCs. Data were quantified as fold-change. *P<0.05, **P<0.01. RE, repetitive element; seq, sequencing; ORF1p, open reading frame 1 protein; ds, double-stranded; BMSCs, Bone marrow mesenchymal stem cells; rJ2, double-stranded RNA clone rJ2; Q, quercetin.

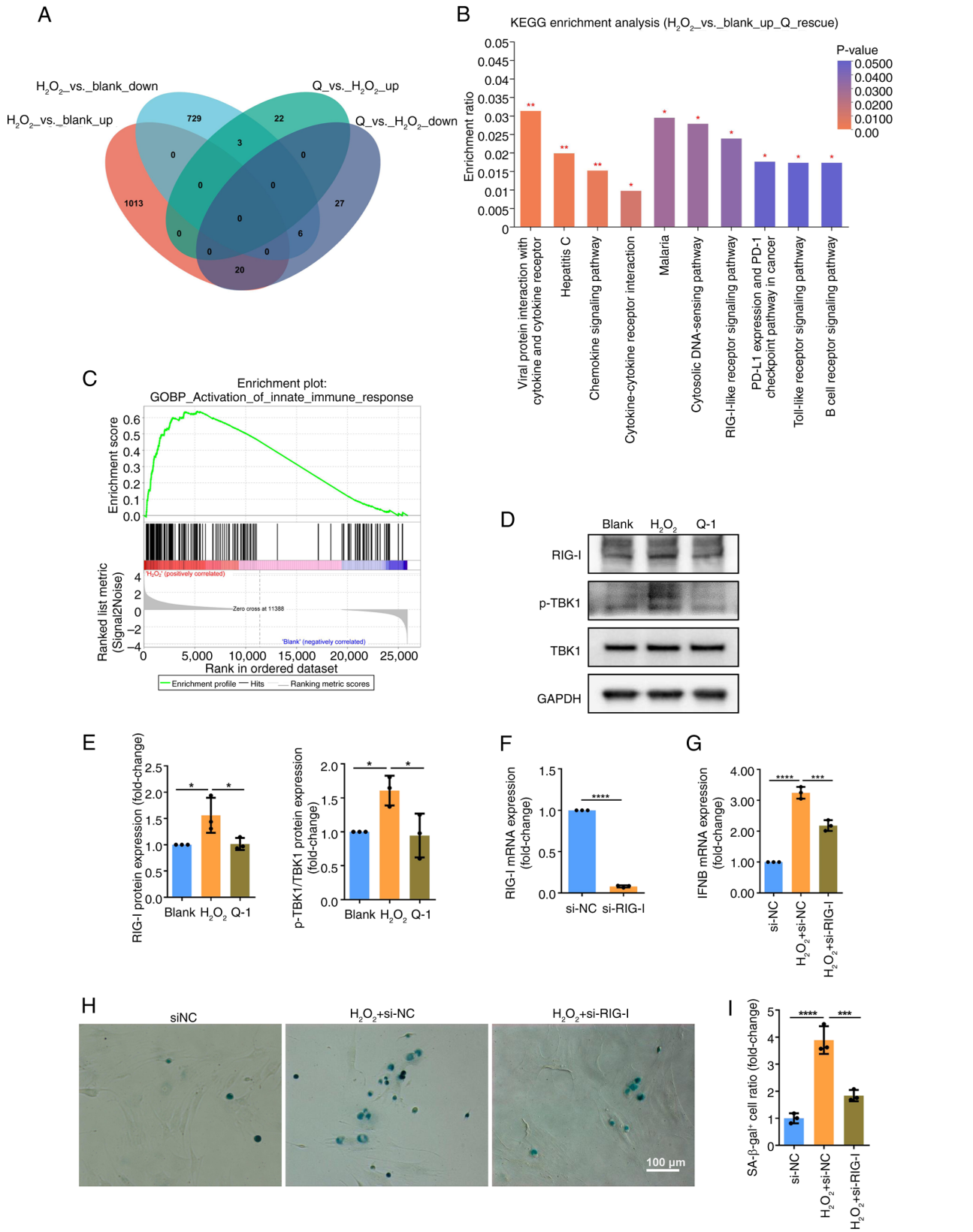

Figure 4. Cytoplasmic double-stranded RNA is recognized by RIG-I-like receptor signaling pathway and initiates innate immune response, leading to senescence of BMSCs. (A) Venn diagram was conducted to identify the genes that showed differential expression following H_2O_2 induction and were subsequently rescued by quercetin. (B) KEGG pathway analysis was used to analyze the differentially expressed genes that were upregulated by H_2O_2 induction and rescued by quercetin. (C) Gene set enrichment analysis was performed to analyze innate immune response (|normalized enrichment score|>1, P<0.05, false discovery rate <0.25). (D) Western blotting was used to assess (E) protein expression of RIG-I, p-TBK1 and TBK1. (F) Validation of RIG-I knockdown efficiency by RT-qPCR and Western blotting. (G) RT-qPCR detected the mRNA expression of IFNB. (H) SA-β-gal staining of BMSCs following H_2O_2 induction and RIG-I knockdown. (I) Proportion of SA-β-gal positive cells was quantified. Data were quantified as fold-change. *P<0.05, ***P<0.001, ****P<0.0001. BMSC, bone marrow mesenchymal stem cell; KEGG, Kyoto Encyclopedia of Genes and Genomes; RIG-1, retinoic acid-inducible gene-1; p-TBK1, phosphorylated TANK-binding kinase 1; SA-β-gal, senescence-associated β-galactosidase; RT-qPCR, reverse transcription-quantitative PCR; siNC, small interfering negative control; Q, quercetin.

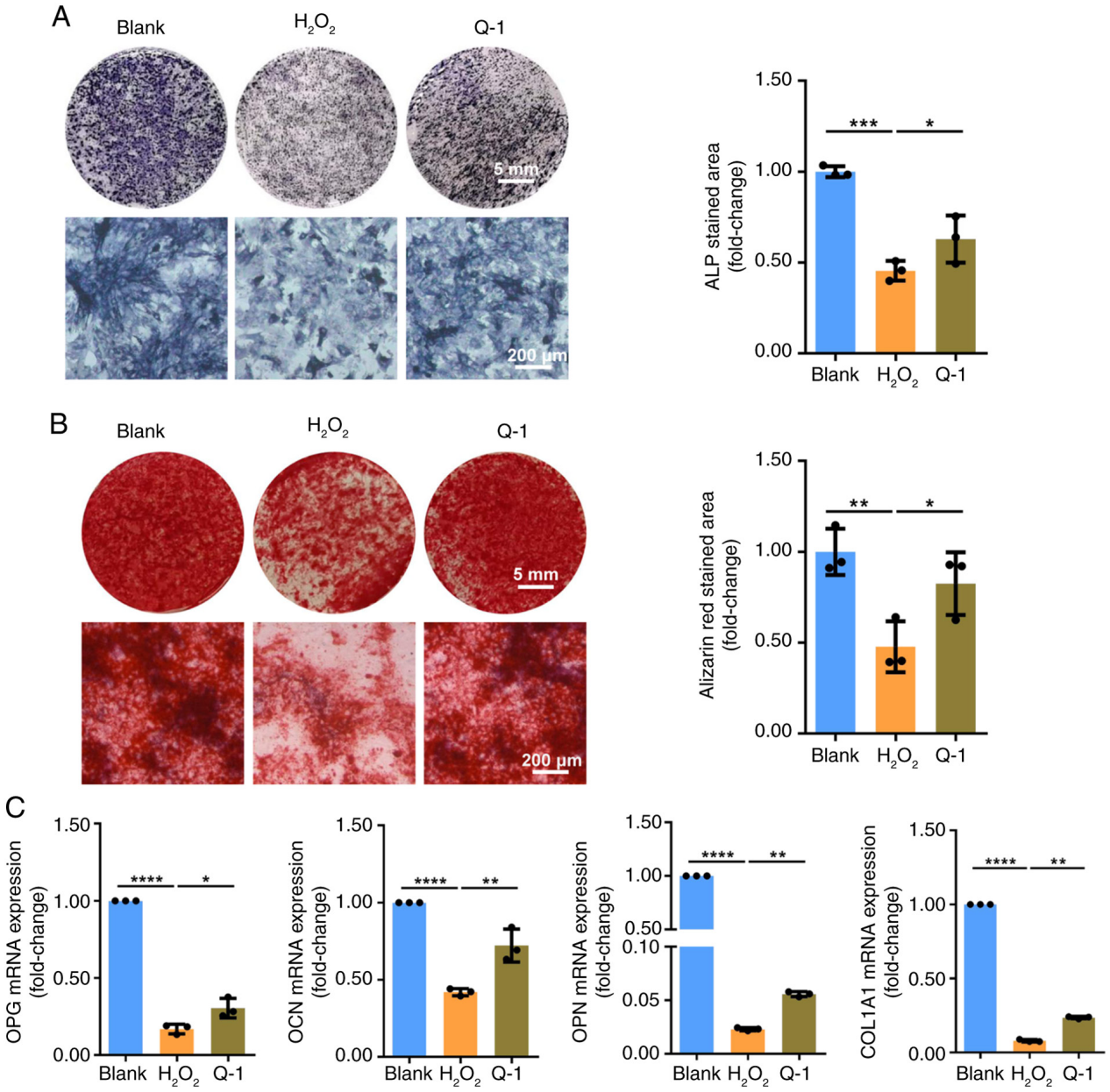

Figure 5. Q restores osteogenic ability of H_2O_2-induced senescent BMSCs. (A) Following 7 days of osteogenic induction, ALP staining was used to evaluate the effect of Q on impaired osteogenic differentiation ability of BMSCs caused by H_2O_2. (B) After 14-21 days of osteogenic induction, alizarin red staining assay was performed. (C) mRNA levels of osteogenic differentiation-related gene including OPG, OCN, OPN and COL1A1 were detected by reverse transcription-quantitative PCR. Data were quantified as fold-change. *P<0.05, **P<0.01 ***P<0.001, ****P<0.0001. OPG, osteoprotegerin; OCN, osteocalcin; OPN, osteopontin; COL1A1, type I collagen A1; BMSC, bone marrow mesenchymal stem cell; ALP, alkaline phosphatase; Q, quercetin.

by H_2O_2 (Fig. 6C). These data indicated that quercetin restored the osteogenic differentiation ability of senescent BMSCs, potentially due to the inhibition of the dsRNA-triggered RIG-I receptor signaling pathway.

Discussion

The senescence of mesenchymal SCs markedly impairs their ability to replicate and differentiate, thereby decreasing their potential for tissue regeneration and repair (2,3). In the present study, epigenomic rearrangements occurred during cellular senescence in BMSCs, as evidenced by a decrease in the expression of heterochromatin-related indicators Hp1α, H3K9me3 and LAP2. This leads to transcriptional activation of REs and subsequent induction of downstream RNA-sensing pathways. Here, quercetin stabilizes heterochromatin, inhibits the release of REs and suppresses the activation of RNA-sensing signaling pathways. As a result, it mitigates oxidative stress-induced senescence in BMSCs and enhances their osteogenic capability.

Retrotransposons have coevolved with their host genomes since the emergence of life (12). Certain beneficial interactions are established during development, such as facilitating necessary chromatin status before implantation in mouse embryos through transcriptional activation of specific LTR and growth LINE-1 elements (31) and using LTR enhancers to regulate key genes involved in human innate immune pathways (32). However, inadvertent activation of retrotransposons in adult

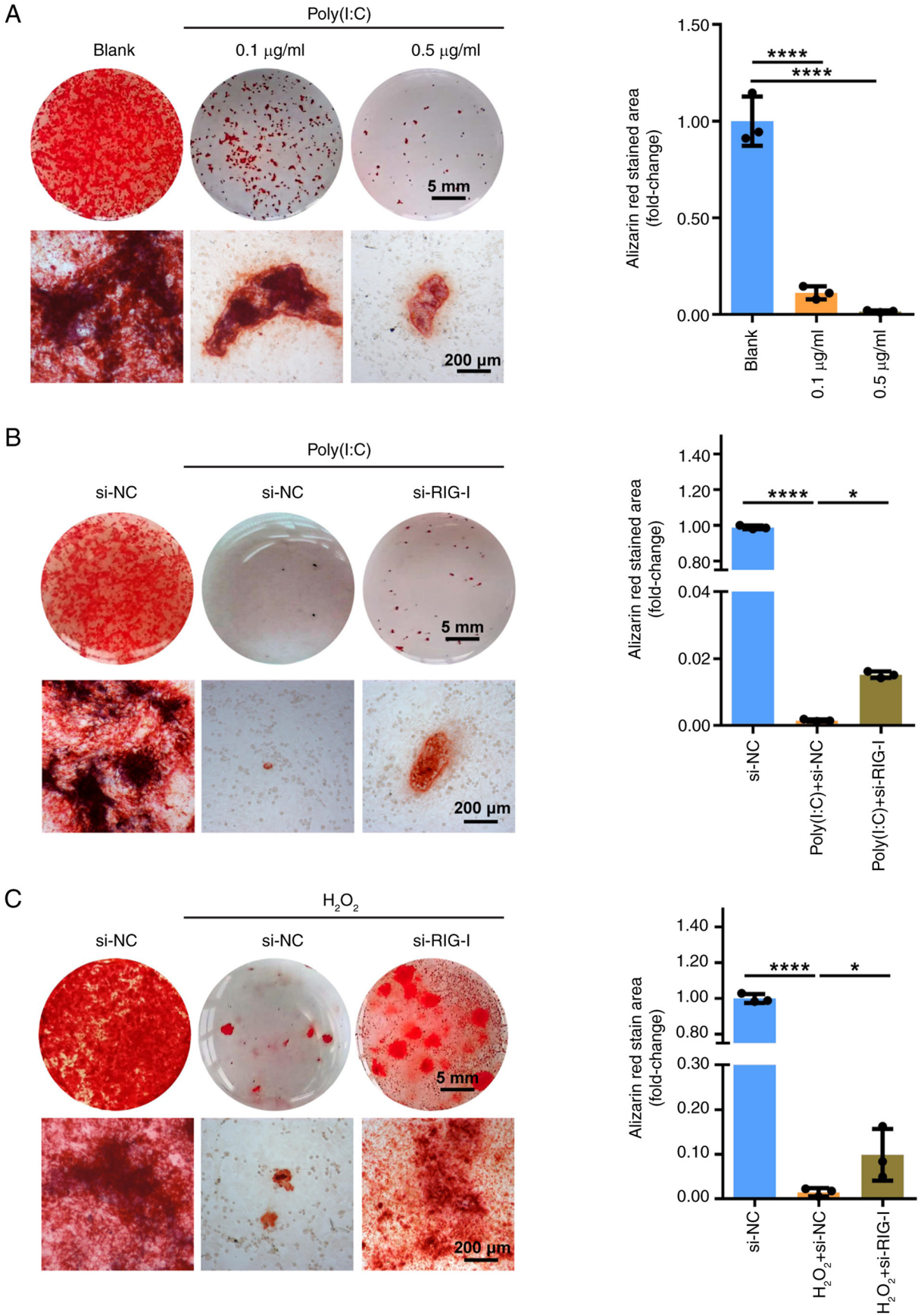

Figure 6. Knockdown of RIG-I rescues the impaired osteogenic ability in senescent BMSCs. (A) BMSCs were stimulated with different concentrations of Poly(I:C) for 24 h, cultured in osteogenic induction medium for 14-21 days and subjected to alizarin red staining. (B) BMSCs were pretreated with 0.1 μg/ml Poly(I:C) for 24 h followed by RIG-I knockdown using siRNA. Following 14-21 days of osteogenic induction, alizarin red staining assay was conducted. (C) BMSCs were pretreated with 200 μM H_2O_2 for 1 h followed by RIG-I knockdown using siRNA. Following 14-21 days of osteogenic induction, alizarin red staining assay was conducted. Data were quantified as fold-change. *P<0.05, ****P<0.0001. RIG-I, retinoic acid-inducible gene I; BMSC, bone marrow mesenchymal stem cell; Poly(I:C), Poly(I:C)-LMW/LyoVec™; siNC, short intefering negative control; Q, quercetin.

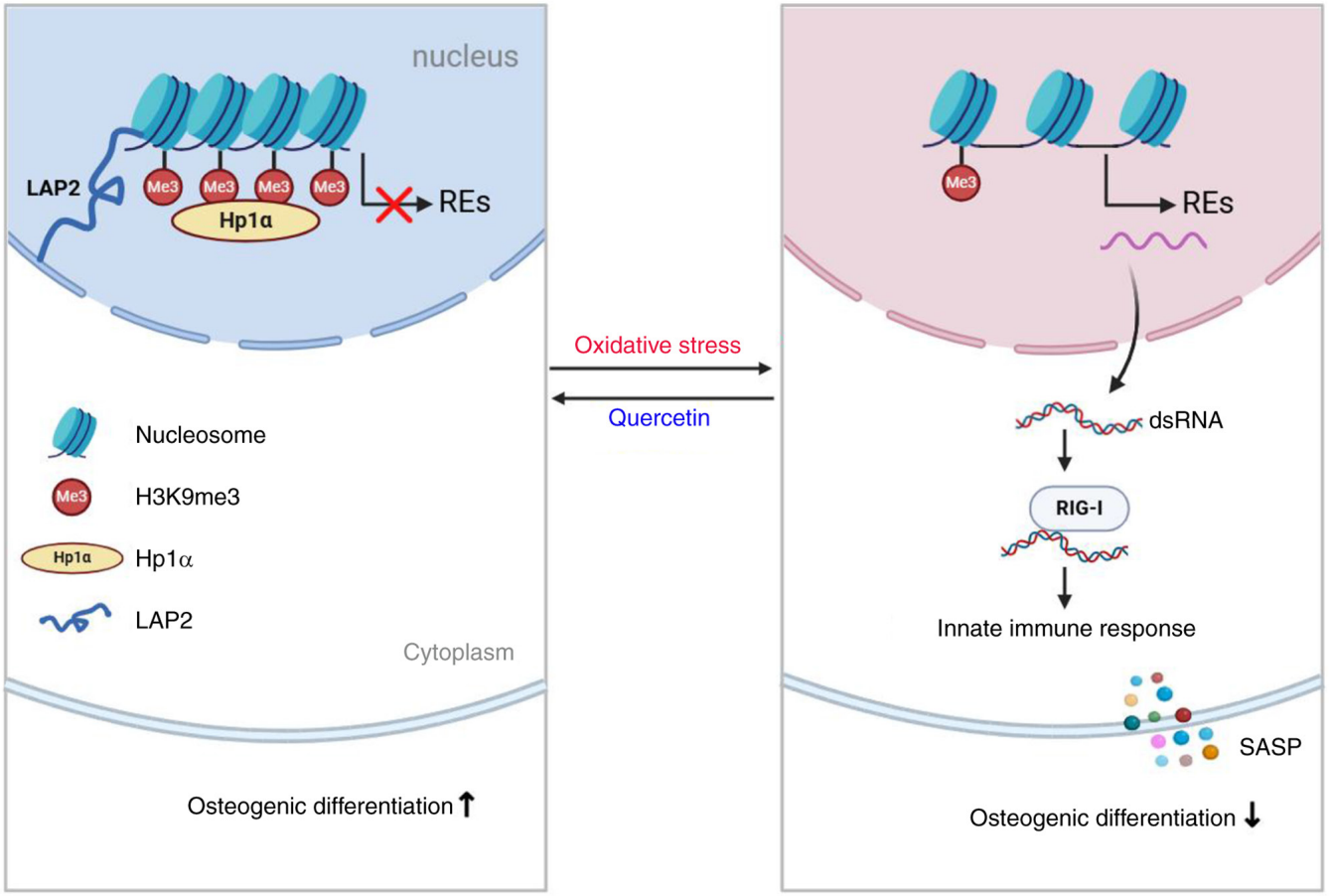

Figure 7. Mechanism by which quercetin ameliorates senescence and promotes osteogenic differentiation of bone marrow mesenchymal stem cells. The epigenetic modifications (H3K9me3, HP1α, and LAP2) undergo changes in the BMSC genome under oxidative stress. This leads to a loss of heterochromatin structure and activation of RE transcription. RE transcripts are released into the cytoplasm, causing an accumulation of dsRNA that triggers RIG-I receptor signaling and activates the innate immune response. Subsequently, proinflammatory cytokines released may function as SASP, promoting BMSC senescence and inhibiting osteogenic differentiation. However, quercetin can effectively stabilize heterochromatin structure, thus alleviating cell senescence and restoring osteogenic differentiation capability.RE, repetitive elements; H3K9me3, trimethylated histone H3 lysine 9; HP1α, heterochromatin protein 1α; LAP2, lamina-associated polypeptide 2; ds, double-stranded; SASP, senescence-associated secretory phenotype; RIG-I, retinoic acid-inducible gene I.

somatic tissue is associated with potential deleterious effects. Both LTR and LINE-1 RNA and protein are upregulated with age in both *Drosophila* (33,34) and mammals, including mice, monkey and human (35,36). Reactivation of LTR and LINE-1 is observed in fibroblasts and keratinocytes in various forms of cellular senescence, including replicative and oncogene- and irradiation-induced senescence (37-39). Here, H_2O_2-induced senescence in BMSCs resulted in the upregulation of LTR and LINE-1. The present data suggested that the reactivation of REs serves a crucial role in stem cell senescence while quercetin reverses this effect.

Retrotransposons are suppressed through a variety of mechanisms, with the most extensively studied being the formation of heterochromatin via epigenetic regulation (8,9,34). This occurs by recruiting chromatin remodeling enzymes and effector proteins to retrotransposon DNA sequences. Levels of heterochromatin or factors involved in establishing heterochromatin decrease with age, leading to an increase in retrotransposon activity (40,41). The present study revealed that markers of heterochromatin such as H3K9me3 and HP1α, along with LAP2, were downregulated following H_2O_2-indcued senescence of BMSCs. Meanwhile, transcripts of LINE-1 and ERVs were upregulated in the present study, indicating that retrotransposons are activated due to epigenetic reset and loss of heterochromatin structure. Administration of quercetin rescues these alterations, suggesting its protective role in stabilizing heterochromatin.

Recently, activation of retrotransposons has been shown to exert a detrimental impact on aging and disease, primarily attributed to recognition of nucleic acids derived from retrotransposons (11,38). dsDNA or dsRNA in the cytoplasm is generally perceived as an intruding pathogen, triggering innate immune pathways (18). Endogenous dsRNA can arise from bidirectional transcription of retrotransposons or through imperfect base pairing of identical or similar elements. These molecules are detected by members of the RIG-I-like receptor family, namely RIG-I, melanoma differentiation-associated protein 5 and laboratory of genetics and physiology 2, which bind mitochondrial antiviral signaling (MAVS) protein. This leads to TBK1 phosphorylation and activation of downstream IFN-I response as well as release of proinflammatory cytokines (15) that promote SASP and cell senescence (42). RE-derived RNA can be converted to dsDNA by endogenous reverse transcriptase activity. Cytoplasmic DNA is sensed by cyclic GMP-AMP synthase, resulting in formation of cyclic GMP-AMP, which subsequently binds to stimulator of IFN

genes thereby initiating innate immune pathways (20). In the present study, the cytoplasmic accumulation of dsRNA in senescent BMSCs was observed, while no dsDNA was detected in the cytoplasm, indicating that REs induced senescence through the dsRNA-mediated RIG-I pathway. Additionally, upregulation of RIG-I and p-TBK1 in senescent BMSCs was revealed. Quercetin effectively decreased cytoplasmic dsRNA aggregation and expression levels of RIG-I and p-TBK1. Moreover, knockdown of RIG-I significantly reversed the senescence of BMSCs and restored the impaired osteogenic function.

There is substantial evidence indicating a notable decline in the osteogenic differentiation capacity of BMSCs with aging, which consequently affects bone regeneration potential (43,44). However, limited research has been conducted on the impact of dsRNA and its activation pathway on stem cell differentiation: The existing studies have yielded conflicting results, highlighting the need for further investigation (45,46). Here, osteogenic differentiation ability of BMSCs was significantly decreased after induction of senescence by H_2O_2 or administration of Poly(I:C), a synthetic dsRNA analogue. However, blocking the RNA sensing pathway via quercetin or knockdown of RIG-I effectively improved the compromised osteogenic differentiation in senescent BMSCs. Lou *et al* (47) demonstrated that overexpression of RIG-I impaired the clonogenicity and osteogenic potential of BMSCs. Overall, involvement of a non-canonical pathway, dsRNA/RIG-I, in the regulation of osteogenic differentiation in BMSCs was elucidated and the underlying regulatory mechanism of quercetin in this signaling cascade was unraveled.

Collectively, the findings of the present study demonstrated that the release of REs during senescence triggered activation of the RIG-I RNA sensing pathway and subsequent downstream innate immune response, resulting in decreased osteogenic capacity of BMSCs. Quercetin restored epigenetic regulation and stabilized heterochromatin, thereby inhibiting release of REs and preventing the decline in osteogenic capacity (Fig. 7). The present study offers novel strategies and targets for alleviating senescence of BMSCs and promoting bone regeneration.

Acknowledgements

Not applicable.

Funding

The present study was supported by National Natural Science Foundation of China (grant nos. 82101015, 82202843 and 82301080), Natural Science Foundation of Guangdong Province (grant nos. 2022A1515012493 and 2024A1515010971) and Basic and Applied Basic Research Foundation of Guangdong Province (grant no. 2023A1515010272).

Availability of data and materials

The data generated in the present study may be found in the Sequence Read Archive under accession number PRJNA1156890 or at the following URL: (https://ncbi.nlm.nih.gov/bioproject/PRJNA1156890).

Authors' contributions

JMP, BC and YTS conceived and designed the experiments. YTS, CYW, LLW, ZHL and JX performed the experiments and analyzed the data. JX, BC and JMP confirm the authenticity of all the raw data. All authors have read and approved the final manuscript.

Ethics approval and consent to participate

All animal experimental procedures were approved by the Institutional Animal Care and Use Committee of Sun Yat-Sen University (Guangzhou, China; approval no. SYSU-IACUC-2024-002262).

Patient consent for publication

Not applicable.

Competing interests

The authors declare that they have no competing interests.

References

1. Zheng C, Chen J, Liu S and Jin Y: Stem cell-based bone and dental regeneration: A view of microenvironmental modulation. Int J Oral Sci 11: 23, 2019.
2. Al-Azab M, Safi M, Idiiatullina E, Al-Shaebi F and Zaky MY: Aging of mesenchymal stem cell: Machinery, markers, and strategies of fighting. Cell Mol Biol Lett 27: 69, 2022.
3. Lin H, Sohn J, Shen H, Langhans MT and Tuan RS: Bone marrow mesenchymal stem cells: Aging and tissue engineering applications to enhance bone healing. Biomaterials 203: 96-110, 2019.
4. Lopez-Otin C, Blasco MA, Partridge L, Serrano M and Kroemer G: The hallmarks of aging. Cell 153: 1194-1217, 2013.
5. Zhang W, Li J, Suzuki K, Qu J, Wang P, Zhou J, Liu X, Ren R, Xu X, Ocampo A, *et al*: Aging stem cells. A Werner syndrome stem cell model unveils heterochromatin alterations as a driver of human aging. Science 348: 1160-1163, 2015.
6. Soto-Palma C, Niedernhofer LJ, Faulk CD and Dong X: Epigenetics, DNA damage, and aging. J Clin Invest 132: e158446, 2022.
7. Pathak RU, Soujanya M and Mishra RK: Deterioration of nuclear morphology and architecture: A hallmark of senescence and aging. Ageing Res Rev 67: 101264, 2021.
8. Stamidis N and Żylicz JJ: RNA-mediated heterochromatin formation at repetitive elements in mammals. EMBO J 42: e111717, 2023.
9. McCarthy RL, Kaeding KE, Keller SH, Zhong Y, Xu L, Hsieh A, Hou Y, Donahue G, Becker JS, Alberto O, *et al*: Diverse heterochromatin-associated proteins repress distinct classes of genes and repetitive elements. Nat Cell Biol 23: 905-914, 2021.
10. Anwar SL, Wulaningsih W and Lehmann U: Transposable Elements in human cancer: Causes and consequences of deregulation. Int J Mol Sci 18: 974, 2017.
11. Gorbunova V, Seluanov A, Mita P, McKerrow W, Fenyö D, Boeke JD, Linker SB, Gage FH, Kreiling JA, Petrashen AP, *et al*: The role of retrotransposable elements in ageing and age-associated diseases. Nature 596: 43-53, 2021.
12. Wang J, Lu X, Zhang W and Liu GH: Endogenous retroviruses in development and health. Trends Microbiol 32: 342-354, 2024.
13. Ågren JA and Clark AG: Selfish genetic elements. PLoS Genet 14: e1007700, 2018.
14. Huang CR, Burns KH and Boeke JD: Active transposition in genomes. Annu Rev Genet 46: 651-675, 2012.
15. Dumetier B, Sauter C, Hajmirza A, Pernon B, Aucagne R, Fournier C, Row C, Guidez F, Rossi C, Lepage C, *et al*: Repeat element activation-driven inflammation: Role of NFκB and implications in normal development and cancer? Biomedicines 10: 3101, 2022.

16. Lanciano S and Cristofari G: Measuring and interpreting transposable element expression. Nat Rev Genet 21: 721-736, 2020.
17. Copley KE and Shorter J: Repetitive elements in aging and neurodegeneration. Trends Genet 39: 381-400, 2023.
18. Gazquez-Gutierrez A, Witteveldt J, Heras SR and Macias S: Sensing of transposable elements by the antiviral innate immune system. RNA 27: 735-752, 2021.
19. Evans TA and Erwin JA: Retroelement-derived RNA and its role in the brain. Semin Cell Dev Biol 114: 68-80, 2021.
20. Miller KN, Victorelli SG, Salmonowicz H, Dasgupta N, Liu T, Passos JF and Adams PD: Cytoplasmic DNA: Sources, sensing, and role in aging and disease. Cell 184: 5506-5526, 2021.
21. Cui Z, Zhao X, Amevor FK, Du X, Wang Y, Li D, Shu G, Tian Y and Zhao X: Therapeutic application of quercetin in aging-related diseases: SIRT1 as a potential mechanism. Front Immunol 13: 943321, 2022.
22. Peng D, Chen L, Sun Y, Sun L, Yin Q, Deng S, Niu L, Lou F, Wang Z, Xu Z, *et al*: Melanoma suppression by quercein is correlated with RIG-I and type I interferon signaling. Biomed Pharmacother 125: 109984, 2020.
23. Nieto M, Konigsberg M and Silva-Palacios A: Quercetin and dasatinib, two powerful senolytics in age-related cardiovascular disease. Biogerontology 25: 71-82, 2024.
24. Livak KJ and Schmittgen TD: Analysis of relative gene expression data using real-time quantitative PCR and the 2(-Delta Delta C(T)) method. Methods 25: 402-408, 2001.
25. Lee SS, Vũ TT, Weiss AS and Yeo GC: Stress-induced senescence in mesenchymal stem cells: Triggers, hallmarks, and current rejuvenation approaches. Eur J Cell Biol 102: 151331, 2023.
26. Ritschka B, Storer M, Mas A, Heinzmann F, Ortells MC, Morton JP, Sansom OJ, Zender L and Keyes WM: The senescence-associated secretory phenotype induces cellular plasticity and tissue regeneration. Genes Dev 31: 172-183, 2017.
27. Korotkov A, Seluanov A and Gorbunova V: Sirtuin 6: Linking longevity with genome and epigenome stability. Trends Cell Biol 31: 994-1006, 2021.
28. Feng JX and Riddle NC: Epigenetics and genome stability. Mamm Genome 31: 181-195, 2020.
29. Padeken J, Methot SP and Gasser SM: Establishment of H3K9-methylated heterochromatin and its functions in tissue differentiation and maintenance. Nat Rev Mol Cell Biol 23: 623-640, 2022.
30. Shevelyov YY and Ulianov SV: The nuclear lamina as an organizer of chromosome architecture. Cells 8: 136, 2019.
31. Cosby RL, Chang NC and Feschotte C: Host-transposon interactions: Conflict, cooperation, and cooption. Genes Dev 33: 1098-1116, 2019.
32. Chuong EB, Elde NC and Feschotte C: Regulatory evolution of innate immunity through co-option of endogenous retroviruses. Science 351: 1083-1087, 2016.
33. Li W, Prazak L, Chatterjee N, Grüninger S, Krug L, Theodorou D and Dubnau J: Activation of transposable elements during aging and neuronal decline in Drosophila. Nat Neurosci 16: 529-531, 2013.
34. Wood JG, Jones BC, Jiang N, Chang C, Hosier S, Wickremesinghe P, Garcia M, Hartnett DA, Burhenn L, Neretti N and Helfand SL: Chromatin-modifying genetic interventions suppress age-associated transposable element activation and extend life span in Drosophila. Proc Natl Acad Sci USA 113: 11277-11282, 2016.
35. De Cecco M, Criscione SW, Peterson AL, Neretti N, Sedivy JM and Kreiling JA: Transposable elements become active and mobile in the genomes of aging mammalian somatic tissues. Aging (Albany NY) 5: 867-883, 2013.
36. Liu X, Liu Z, Wu Z, Ren J, Fan Y, Sun L, Cao G, Niu Y, Zhang B, Ji Q, *et al*: Resurrection of endogenous retroviruses during aging reinforces senescence. Cell 186: 287-304.e26, 2023.
37. Colombo AR, Elias HK and Ramsingh G: Senescence induction universally activates transposable element expression. Cell Cycle 17: 1846-1857, 2018.
38. Di Giorgio E, Ranzino L, Tolotto V, Dalla E, Burelli M, Gualandi N and Brancolini C: Transcription of endogenous retroviruses in senescent cells contributes to the accumulation of double-stranded RNAs that trigger an anti-viral response that reinforces senescence. Cell Death Dis 15: 157, 2024.
39. Touma F, Lambert M, Martinez Villarreal A, Gantchev J, Ramchatesingh B and Litvinov IV: The ultraviolet irradiation of keratinocytes induces ectopic expression of LINE-1 retrotransposon machinery and leads to cellular senescence. Biomedicines 11: 3017, 2023.
40. De Cecco M, Ito T, Petrashen AP, Elias AE, Skvir NJ, Criscione SW, Caligiana A, Brocculi G, Adney EM, Boeke JD, *et al*: L1 drives IFN in senescent cells and promotes age-associated inflammation. Nature 566: 73-78, 2019.
41. Wood JG, Hillenmeyer S, Lawrence C, Chang C, Hosier S, Lightfoot W, Mukherjee E, Jiang N, Schorl C, Brodsky AS, *et al*: Chromatin remodeling in the aging genome of Drosophila. Aging Cell 9: 971-978, 2010.
42. Pérez-Mancera PA, Young ARJ and Narita M: Inside and out: The activities of senescence in cancer. Nat Rev Cancer 14: 547-558, 2014.
43. Hu M, Xing L, Zhang L, Liu F, Wang S, Xie Y, Wang J, Jiang H, Guo J, Li X, *et al*: NAP1L2 drives mesenchymal stem cell senescence and suppresses osteogenic differentiation. Aging Cell 21: e13551, 2022.
44. Xie Y, Han N, Li F, Wang L, Liu G, Hu M, Wang S, Wei X, Guo J, Jiang H, *et al*: Melatonin enhances osteoblastogenesis of senescent bone marrow stromal cells through NSD2-mediated chromatin remodelling. Clin Transl Med 12: e746, 2022.
45. Niepmann ST, Willemsen N, Boucher AS, Stei M, Goody P, Zietzer A, Bulic M, Billig H, Odainic A, Weisheit CK, *et al*: Toll-like receptor-3 contributes to the development of aortic valve stenosis. Basic Res Cardiol 118: 6, 2023.
46. Khokhani P, Rahmani NR, Kok A, Öner FC, Alblas J, Weinans H, Kruyt MC and Croes M: Use of therapeutic pathogen recognition receptor ligands for osteo-immunomodulation. Materials (Basel) 14: 1119, 2021.
47. Lou Q, Jiang K, Xu Q, Yuan L, Xie S, Pan Y, Chen J, Wu J, Zhu J, Jiang L and Zhao M: The RIG-I-NRF2 axis regulates the mesenchymal stromal niche for bone marrow transplantation. Blood 139: 3204-3221, 2022.